

DYNAMIC STABILIZATION OF L_2 PERIODIC ORBITS USING ATTITUDE-ORBIT COUPLING EFFECTS¹

Martin Lara (1), Jesús Peláez (2), Claudio Bombardelli (2), Fernando R. Lucas (2), Manuel Sanjurjo-Rivo (3), Davide Curreli (4), Enrico C. Lorenzini (4), Daniel J. Scheeres (5)

(1) *Real Observatorio de la Armada, 11110 San Fernando, Spain, +34 956 545 612, mlara@roa.es*

(2) *Universidad Politécnica de Madrid, 28040 Madrid, Spain, +34 913 366 306, j.pelaez@upm.es, claudio.bombardelli@upm.es, fernando.rodriguez.lucas@gmail.com*

(3) *GMV Aerospace and Defence, 28760 Madrid, Spain, +34 918 072 100, msanrivo@gmail.com*

(4) *University of Padova, 35131 Padova, Italy, +39 049 827 6766, davide.curreli@unipd.it, enrico.lorenzini@unipd.it*

(5) *University of Colorado at Boulder, Boulder, Colorado 80309, USA, +1 303 492 7420, scheeres@colorado.edu*

Abstract: *Numerical explorations show how the known periodic solutions of the Hill problem are modified in the case of the attitude-orbit coupling that may occur for large satellite structures. We focus on the case in which the elongation is the dominant satellite's characteristic and find that a rotating structure may remain with its largest dimension in a plane parallel to the plane of the primaries. In this case, the effect produced by the non-negligible physical length is dynamically equivalent to the perturbation produced by an oblate central body on a mass-point satellite. Based on this, it is demonstrated that the attitude-orbital coupling of a long enough body may change the dynamical characteristics of a periodic orbit about the collinear Lagrangian points.*

Keywords: *roto-orbital dynamics, Hill problem, periodic orbits, stability*

1 Introduction

In the three-bodies problem setting, libration points are places where the gravitational forces exerted by the primaries on the third body counterbalance dynamical forces acting on it. Therefore, the position of a satellite placed on a libration point remains stationary relative to the primaries. From the five libration points the so-called L_2 point, which is collinear with the primaries and beyond the smaller one, has been pointed out to provide superior opportunities for scientific and exploration missions [1]. Specifically, the sun-Earth collinear points are the location chosen for programmed astronomical observatories as ESA's Gaia² or NASA's James Space Web Telescope³.

One drawback of libration point missions is the severe demand of active control stemmed from the inherent instability of the dynamics about the collinear points. Different techniques have been developed to make less severe the stationkeeping requirements [2, 3], including near propellant-free propulsion [4] and the possibility of a purely dynamical stabilization [5]. Here we explore the possibilities of using the attitude-orbit coupling effects to find stabilizing configurations for large space structures where the elongation is the dominant satellite's characteristic.

¹This work reflects research conducted under ESTEC Contract 21259/07/NL/CB for the European Space Agency

²<http://gaia.esa.int/>

³<http://www.jwst.nasa.gov/>

To get a clear insight in the coupled dynamics we simplify the three-bodies dynamics to the Hill problem approximation and only consider elongated objects that are modeled in the dumbbell approximation. Furthermore, for bodies in fast rotation when compared to the rotation rate of the primaries the problem evolves in different time scales, which allows us for carrying an averaging procedure out.

The averaging decouples the rotational motion, which can be integrated analytically in closed form, from the orbital one. Then, the orbital motion is reduced to a time-dependent three degrees of freedom problem in which the satellite's dimension is modeled with a single parameter. In particular, the averaged rotational motion reduces to an equilibria when the fast rotation occurs in a plane parallel to the orbital plane of the primaries. In this case, the orbital motion is conservative and can be explored with the usual tools of nonlinear dynamics. More precisely, the numerical continuation of periodic orbits about L_2 allows us to carry out a systematic study of their dynamic characteristics that shows the influence of the elongation in the orbital dynamics.

2 Hill problem dynamics

The Hill problem is a simplification of the three-body problem, which in turn is a simplification of real models. The three-body problem considers the motion of three point masses under their mutual gravitational attraction. In the “restricted” approximation, it is assumed that the mass of one body, the “secondary”, is so small that it does not influence the motion of the other two bodies called the “primaries”. The “circular” restricted three-body problem (CRTBP) assumes that the primaries evolve in circular orbits around their mutual center of mass. Finally, the Hill problem further simplifies the CRTBP by assuming that the mass m of the primary at the origin (the central body) is small when compared to the mass M of the other primary, and the distance between the primaries l is large when compared to the distance of the secondary to the origin.

The Hill problem provides a good approximation to the real dynamics of a variety of systems. Moreover, the Hill problem assumptions allow for multiplying the time for the rotation rate of the primaries ω to obtain a non-dimensional time scale, and dividing the lengths by $(Gm/\omega^2)^{1/3}$, where Gm is the gravitational constant of the central body. This non-dimensioning process results in an invariant model that does not depend on any physical parameter, hence giving broad generality to the results, which are naturally parametrized by the Jacobi constant C and whose application at different systems becomes a simple matter of scaling.

In the Hill problem scaling the collinear points are placed at the positions $(\pm\rho_H, 0, 0)$, where $\rho_H = 3^{-1/3}$ is the Hill radius. They are equilibria of the differential system that are known to be unstable. Besides the equilibria solutions, periodic orbits are particular solutions of specific interest because they are the only solutions which evolution is known for all time. Furthermore, the stability character of a periodic orbit can be easily ascertained by integrating its variational equations.

Periodic solutions of the Hill problem are not isolated, but grouped in “natural” families of periodic orbits generated by variations of the Jacobi constant. Basic families start with small oscillations around the central body or the collinear points. From the basic families of periodic orbits new families appear as branches that bifurcate at different “critical” orbits (orbits with indifferent stability character) either in the plane of the primaries or out of it.

The stability of a periodic orbit is derived from the eigenvalues of the state transition matrix at the end of one period. To the aims of this work, we just mention that the linear stability character is described by two indices, say k_1 and k_2 , such that the condition $k_{1,2}$ real and $|k_{1,2}| < 2$ applies for linear stability, critical orbits occurring when either k_1 or k_2 are $|2|$. Then, stability curves that show

the pattern of these indices parametrized by the Jacobi constant provide a crucial information on the stability evolution of a given family of periodic orbits.

We only pay attention to two among the variety of families of periodic orbits of the Hill problem that are known to exist for variations of the Jacobi constant [6, 7]. These are the family of 8-shaped periodic orbits, which starts from small vertical oscillations through the L_2 collinear point, and the family of Halo orbits, which bifurcates from the family of Lyapunov orbits that starts from small retrograde oscillations in the plane of the primaries about L_2 . The description of these families is taken from [5] where more detail is provided as well as the description of other families.

2.1 Eight-shaped orbits of the Hill problem

The family of eight-shaped periodic orbits of the Hill problem starts with small vertical oscillations through the collinear points. Decreasing values of the Jacobi constant produce eight-shaped orbits of increasing size and period. The orbits of this family are symmetric with respect to the planes $\zeta = 0$ and $\eta = 0$, and cross the plane $\zeta = 0$ only at $\eta = 0$ and $\xi = 0$. Three sample orbits of this family are presented in the left plot of Fig. 1 for, from larger to smaller, $C = 0, 1$, and 2.

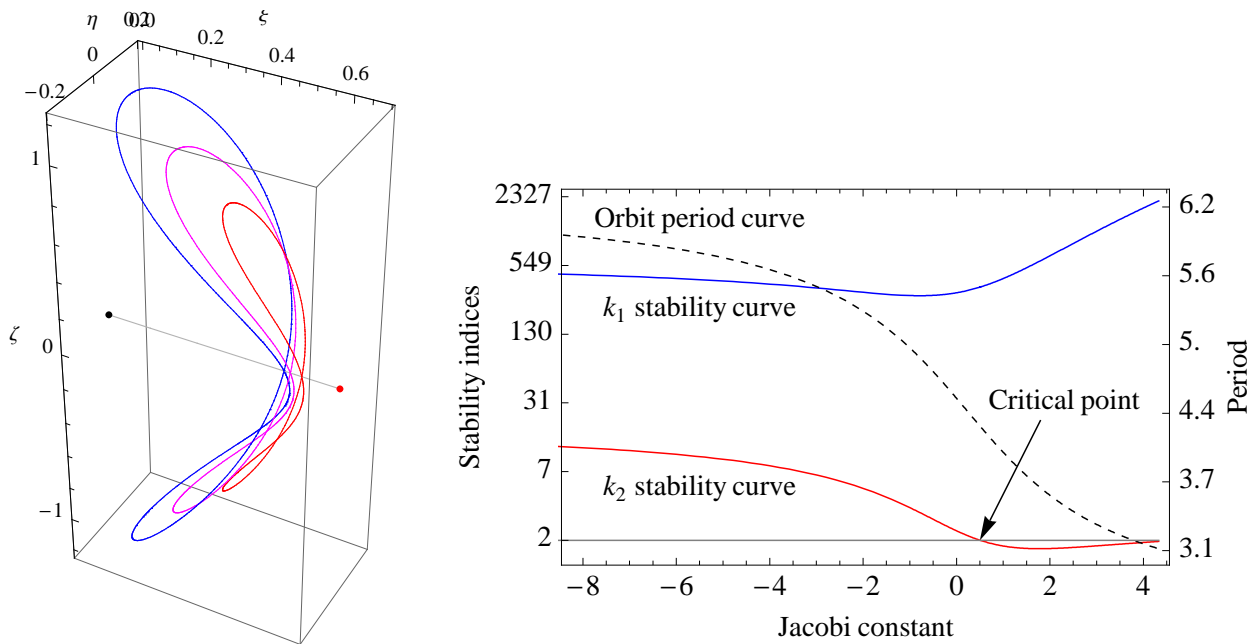


Figure 1: *Left: sample eight-shaped orbits for $C = 2$ (red), 1 (magenta), and 0 (blue). The black and red dots joined with a straight line mark the central body and the L_2 point, respectively. Right: stability-period diagram of the family of eight-shaped periodic orbits of the Hill problem.*

The family of eight-shaped orbits of the Hill problem is made of highly unstable orbits with one of the stability indices, say k_1 , always having very high values. As shown in the right plot of Fig. 1, the stability index k_1 first decreases with C until the Jacobi constant takes the value $C = -0.78757$ ($k_1 = 361.252$) and then continuously grows. The other stability index starts with small values (the minimum $k_2 = 1.63823$ occurs at $C = 1.76243$), but soon it crosses the critical value $k_2 = +2$ at $C = 0.512431$, where the corresponding value of the other index is $k_1 = 434.131$, and then grows continuously although with moderate values. Note that the ordinates are represented in the usual hyperbolic arcsin scale.

2.2 Halo orbits of the Hill problem

The family of Halo orbits starts from a critical bifurcation orbit of the family of Lyapunov orbits at $C = 4.00531$, where the period is $T = 3.08144$. Figure 2 shows the stability-period diagram of the family of Halo orbits (left plot) and one sample stable orbit (right plot). The family starts with a highly unstable, planar Lyapunov orbit and for decreasing values of the Jacobi constant the orbits move from the L_2 point towards the origin with increasing inclination with respect to the plane of the primaries. The period of the Halo orbits, represented with a dashed curve in the left plot of Fig. 2, monotonously decreases along the family.

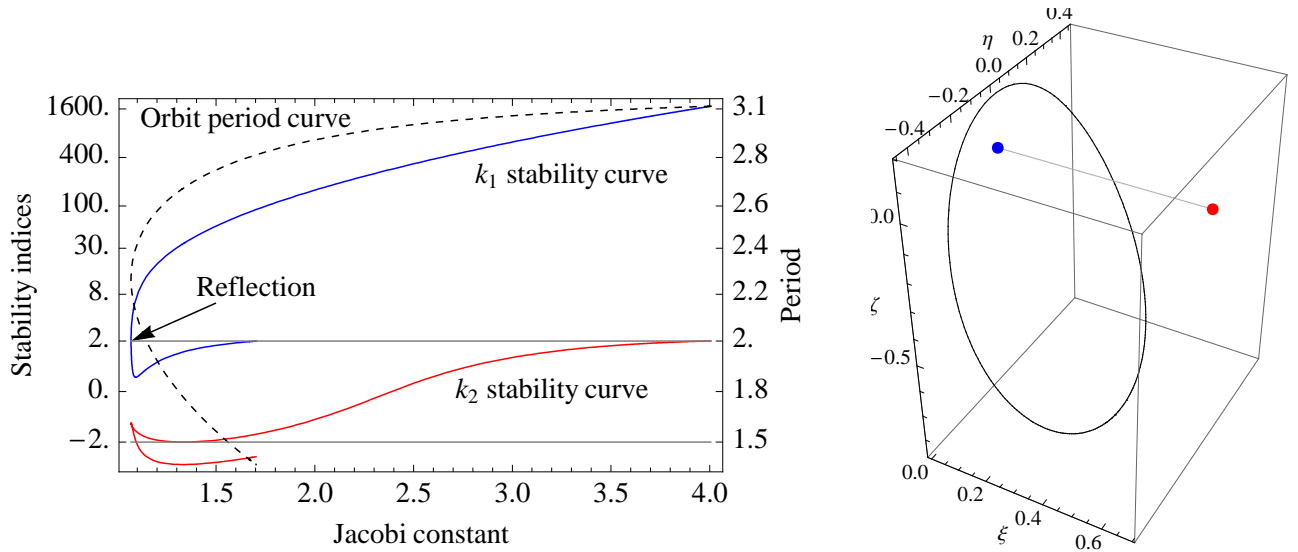


Figure 2: *Left: stability-period diagram of the family of Halo orbits of the Hill problem. Right: sample stable orbit for $C = 1.08$ (the blue and red dots linked by a gray line are the origin and L_2 point, respectively).*

The instability of the Halo orbits becomes smaller and smaller until finding a reflection orbit at $C = 1.06903$. After the reflection, Halo orbits exist for increasing values of the Jacobi constant, and enjoy linearly stable character in a short region until changing again to instability at $C = 1.09515$. It is known that this family continues with orbits that get closer and closer to the origin until its termination in a collision orbit.

Finally, we note that, because of the symmetries of the Hill problem, for any three-dimensional solution there exists also a symmetric orbit with respect to the plane of the primaries.

3 Dumbbell satellite in fast rotation

In the Hill problem scaling $\boldsymbol{\rho} \equiv (\xi, \eta, \zeta)$ are the coordinates of the center of mass of an extended satellite, whose attitude is described by the orientation of the unit vector in the direction of the dumbbell length with respect to the Hill problem frame. We find convenient to use the Bryant angles (ϕ_1, ϕ_2, ϕ_3) for describing this orientation. When the attitude rotation of the dumbbell is much faster than the rotation rate of the system, the case of a fast rotating dumbbell, the attitude evolution can be studied in the long-term by averaging the equations over the “fast angle” ϕ_3 . Then, it can be shown

that the attitude motion decouples from the orbital motion [5]. Thus,

$$\phi_1' = \cos \phi_1 \tan \phi_2, \quad \phi_2' = -\sin \phi_1 \quad (1)$$

where ‘‘primes’’ mean derivative in the non-dimensional time scale. Equations (1) can be integrated analytically, showing that, on average, the rotational angular momentum keeps a constant direction in the inertial space and, therefore, it rotates with constant rate $-\omega$ in the synodic frame.

After integrating Eqs. (1), the orbital motion is obtained from the integration of

$$\xi'' - 2\eta' = 3\xi - \frac{\xi}{\rho^3} + \frac{\ell^2}{\rho^5} \left[\frac{3}{2} \left(5 \frac{\Delta^2}{\rho^2} - 1 \right) \xi - 3\Delta \sin \phi_2 \right] \quad (2)$$

$$\eta'' + 2\xi' = -\frac{\eta}{\rho^3} + \frac{\ell^2}{\rho^5} \left[\frac{3}{2} \left(5 \frac{\Delta^2}{\rho^2} - 1 \right) \eta + 3\Delta \cos \phi_2 \sin \phi_1 \right] \quad (3)$$

$$\zeta'' = -\zeta - \frac{\zeta}{\rho^3} + \frac{\ell^2}{\rho^5} \left[\frac{3}{2} \left(5 \frac{\Delta^2}{\rho^2} - 1 \right) \zeta - 3\Delta \cos \phi_2 \cos \phi_1 \right] \quad (4)$$

where $\rho = \|\boldsymbol{\rho}\|$, $\Delta = \xi \sin \phi_2 - (\eta \sin \phi_1 - \zeta \cos \phi_1) \cos \phi_2$ is a non-dimensional auxiliary distance, and we introduce the non-dimensional parameter

$$\ell = \sqrt{\frac{a_2}{2}} \frac{L/l}{\nu^{1/3}}, \quad (5)$$

where L/l is the ratio of the satellite’s physical length to the distance between the primaries, $\nu = m/(m + M)$ is the reduced mass of the central body, and a_2 is a non-dimensional coefficient related to the satellite’s mass distribution such that $0 < 4a_2 < 1$, cf. [5]. In the case $\ell = 0$, of course, Eqs. (2)–(4) recover the classical Hill equations. The parameter ℓ captures the influence of the dumbbell’s length in the dynamics, and we call it the satellite’s *characteristic length*. Full details on the derivation of these equations can be found in [5].

Therefore, for given initial conditions, the long-term evolution of fast rotating dumbbell satellites is reduced to a time-dependent three degrees of freedom problem given by Eqs. (2)–(4) in which the attitude solution of Eq. (1) must be replaced.

For the initial conditions $\phi_1 = \phi_2 = 0$, Eqs. (1) identically vanish and the dumbbell evolves, on average, with constant attitude parallel to the plane of the primaries. For this attitude-equilibrium configuration $\Delta = \zeta$ and the motion of the center of mass is obtained from

$$\xi'' - 2\eta' = 3\xi - \frac{\xi}{\rho^3} - \frac{3}{2} \ell^2 \frac{\xi}{\rho^5} \left(1 - 5 \frac{\zeta^2}{\rho^2} \right), \quad (6)$$

$$\eta'' + 2\xi' = -\frac{\eta}{\rho^3} - \frac{3}{2} \ell^2 \frac{\eta}{\rho^5} \left(1 - 5 \frac{\zeta^2}{\rho^2} \right), \quad (7)$$

$$\zeta'' = -\zeta - \frac{\zeta}{\rho^3} - \frac{3}{2} \ell^2 \frac{\zeta}{\rho^5} \left(3 - 5 \frac{\zeta^2}{\rho^2} \right), \quad (8)$$

equations that admit the Jacobi constant

$$C = 3\xi^2 - \zeta^2 + \frac{2}{\rho} + \frac{\ell^2}{\rho^2} \left(1 - \frac{3\zeta^2}{\rho^2} \right) - (\xi'^2 + \eta'^2 + \zeta'^2).$$

A notable result of Eqs. (6)–(8) is that they are formally equal to the well known equations of the Hill-oblolate problem: a Hill’s problem perturbed by the oblateness of a central body. In the fast-rotating dumbbell problem, the role of the oblateness is played by $\ell^2 \equiv J_2 \alpha^2$, where α is the equatorial radius of the central body and J_2 is the second order zonal harmonic coefficient. Therefore, in what respects to the orbital motion of the center of mass, the effect of a non-negligible dumbbell’s length is analogous to that produced by the non-sphericity of the central body.

4 Numerical explorations

As the orbital problem given by Eqs. (6)–(8) is conservative, the standard search for periodic orbits and their analytic continuation provides a great insight in the dynamics. Below we provide two sample cases taking the characteristic length as the parameter generator of the families. The description of these families is taken from [5] where more detail is provided as well as the description of other families.

Usual procedures for the continuation of families of periodic orbits rest upon the computation of differential corrections that require the integration of the variational equations. These are

$$\begin{aligned}\delta\xi'' &= 3\delta\xi - \sigma^2(\sigma\delta\xi + 3\xi\delta\sigma) + 5\ell^2\sigma^4\xi S_2\delta\sigma + \ell^2\sigma^5(S_2\delta\xi + \xi\delta S_2) + 2\delta\eta' + \lambda\sigma^5\xi S_2 \\ \delta\eta'' &= -\sigma^2(\sigma\delta\eta + 3\eta\delta\sigma) + 5\ell^2\sigma^4\eta S_2\delta\sigma + \ell^2\sigma^5(S_2\delta\eta + \eta\delta S_2) - 2\delta\xi' + \lambda\sigma^5\eta S_2 \\ \delta\zeta'' &= -\delta\zeta - \sigma^2(\sigma\delta\zeta + 3\zeta\delta\sigma) + 5\ell^2\zeta\sigma^4(S_2 - 3)\delta\sigma + \ell^2\sigma^5[(S_2 - 3)\delta\zeta + \zeta\delta S_2] + \lambda\sigma^5\zeta(S_2 - 3)\end{aligned}$$

where

$$\sigma = \frac{1}{\rho}, \quad \delta\sigma = -\sigma^3(\xi\delta\xi + \eta\delta\eta + \zeta\delta\zeta), \quad S_2 = -\frac{3}{2}(1 - 5\zeta^2\sigma^2), \quad \delta S_2 = 15\zeta\sigma(\sigma\delta\zeta + \zeta\delta\sigma),$$

and $\lambda \equiv 1$ for length variations while $\lambda \equiv 0$ for Jacobi constant variations. Note that for length variations we choose the square of the characteristic length as the parameter because it always appears in the equations as ℓ^2 .

We note that periodic orbits are not limited to the equilibrium case of constant attitude motion of Eqs. (6)–(8), and may survive in the non-conservative case described by Eqs. (2)–(4). However, the periodic orbits are no longer grouped in families for variations of the Jacobi constant and only isolated 2π -periodic orbits may exist because the explicit appearance of time in the equations of motion. An account of the time-dependent case of non-constant attitude can be found in [5, 8].

4.1 Eight-shaped orbits of the fast-rotating dumbbell problem

Despite the clear instability of the eight-shaped orbits of the Hill problem that can be appreciated in Fig. 1, variations of the characteristic length make it possible, in general, to find orbital stability. This is not true, however, for eight-shaped orbits with values of the Jacobi constant above say $C \approx 3$ (cf. [5]). Besides the effects on stability produced by characteristic length variations, the shape and size of the orbit is also affected, which moves and curves towards the origin. As an example, below we provide the family for $C = 2$, where we find two stability regions separated by a region of complex instability.

The family of eight-shaped periodic orbits of the fast-rotating dumbbell problem with constant $C = 2$, starts with a highly unstable orbit of the Hill problem ($\ell^2 = 0$). Increasing the characteristic length

produces orbits of smaller size and period, which reduce their instability character (see Fig. 3). One of the stability indices, say k_1 , reduces continuously while the other slightly increases. The period reduces when increasing the characteristic length until a minimum that occurs at $\ell^2 = 0.109415$, after which a reflection of the family over the period occurs, and periodic orbits exist with increasing period.

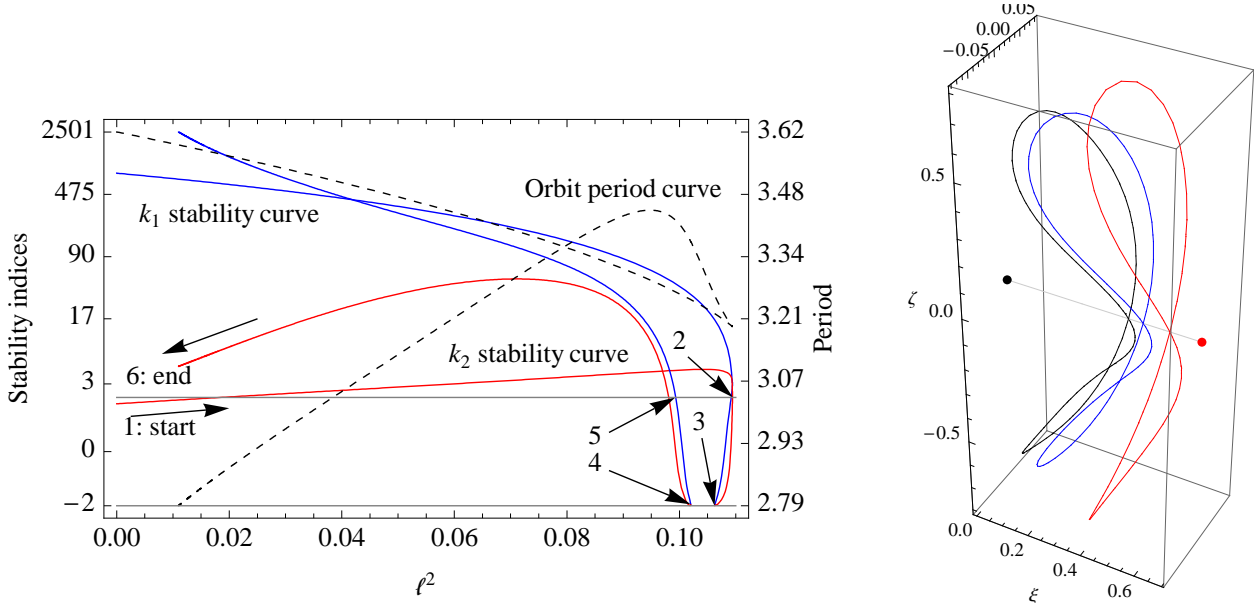


Figure 3: *Left: stability-period diagram of a family of eight-shaped, periodic orbits with constant $C = 2$ for characteristic length variations; the horizontal gray lines correspond to the critical values $k = \pm 2$. Right: stable orbits for $\ell^2 = 0.1$ (left) $\ell^2 = 0.1075$ (center), and unstable orbit of the Hill problem ($\ell^2 = 0$, right); note the different scale for the η -axis.*

Very close to the value of ℓ for which the reflection in the period occurs, we find maximum characteristic length $\ell^2 = 0.109416$ for which periodic orbits of this family exist (point 2 in the left plot of Fig. 3). Periodicity is broken for higher values of ℓ^2 , but, after a reflection in ℓ , the family can be continued for decreasing values of the characteristic length.

The reflected branch of the family is made of orbits that immediately enter a region of stability at $\ell^2 = 0.109203$. Further decreasing the characteristic length produces stable orbits until $\ell^2 = 0.106275$ (point 3 in the left plot of Fig. 3), where the dumbbell enters a region of complex instability. At $\ell^2 = 0.101998$ (point 4 in the left plot of Fig. 3) the satellite enters another stability region, and the stability character changes again to instability at $\ell^2 = 0.0993536$ (point 5 in the left plot of Fig. 3). Very close to this value of ℓ a new reflection in the period occurs, and periodic orbits of this family exist with shorter periods, reaching high instability values for decreasing values of the characteristic length.

The right plot of Fig. 3 shows three sample orbits of this family. The higher one (the rightmost, in red) is the starting orbit, a highly unstable eight-shaped orbit of the Hill problem ($\ell = 0$) with $C = 2$. The other two are stable orbits, one from each stability region, with characteristic length $\ell^2 = 0.1$ (left) and $\ell^2 = 0.1075$ (center).

Table 1 provides the initial conditions of some critical orbits of this family, where the ‘‘Type’’ of the stability indices is noted **R** for real k_1 and k_2 stability indices and **C** for complex conjugate indices, $k_1 \equiv \Re(k)$, $k_2 \equiv |\Im(k)|$. Numbers in typewriter style in the tables’ caption make reference to corresponding points in the stability-period diagram in the left plot of Fig. 3.

4.2 Halo orbits of the fast-rotating dumbbell problem

Increasing the characteristic length of a dumbbell in an Halo orbit tends to improve its orbital stability characteristics, in general, even finding stability in some cases. Again, variations of the characteristic length modify the size and shape of the orbit, and its relative position with respect to the origin. However, once a stable orbit has been found for a certain characteristic length, variations of the Jacobi constant might maintain stability while slightly changing other orbit's characteristics.

For low values of the Jacobi constant, say $C \leq 1.5$, the general behavior of the families of Halo orbits of the fast-rotating dumbbell problem with constant C for variations of ℓ is to link two different unstable orbits of the family of Halo orbits of the Hill problem. Thus, the families start from a stable Halo orbit of the Hill problem ($\ell = 0$); increasing the characteristic length leads to a reflection and, then, decreasing the characteristic length links the stable Halo orbit of the Hill problem with the unstable one that exists for the same value of the Jacobi constant (cf. Fig. 2). The link-families find stability in between for relatively small characteristic lengths.

As an example, we provide the stability-period diagram of the family for $C = 1.2$ in the left plot of Fig. 4. The right plot of Fig. 4 shows three sample orbits. The initial conditions of the starting, reflection, and termination orbit of this family are given in table 2.

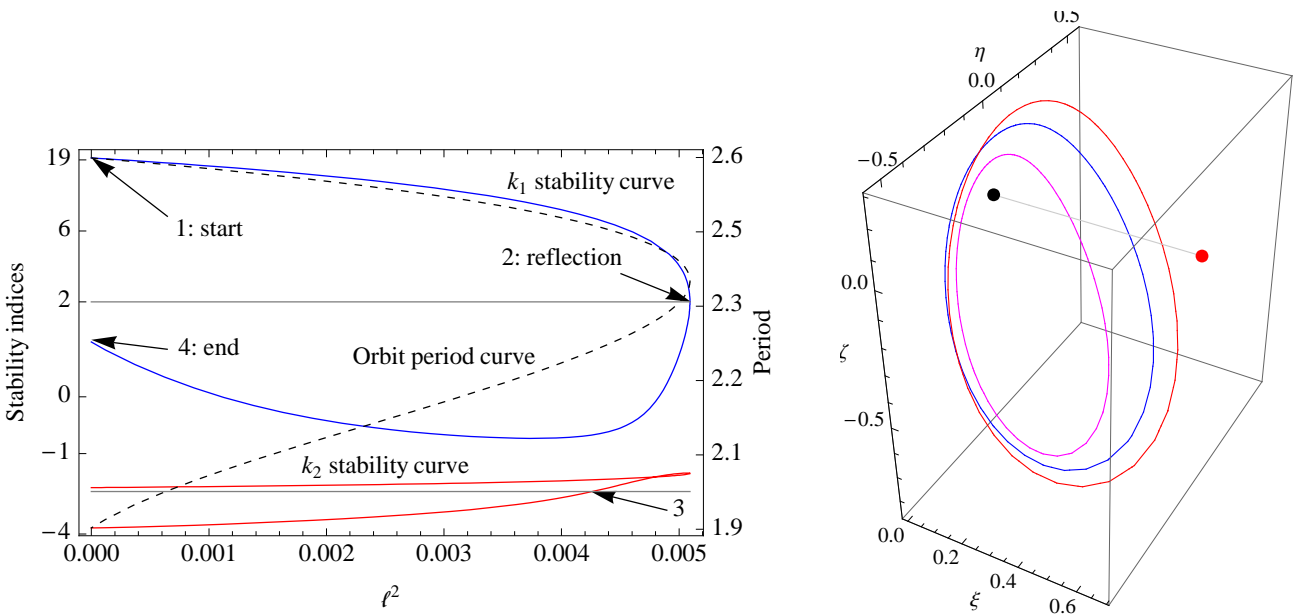


Figure 4: *Stability-period diagram of the family of Halo orbits with $C = 1.2$ for variations of the characteristic length. Right: unstable Halo orbits of the Hill problem (red and magenta) and stable (blue) Halo orbit with $\ell^2 = 0.0045$.*

Starting from higher values of the Jacobi constant results in a quite different behavior. Although stability regions still may be found they occur at higher values of ℓ . On the contrary, the more unstable Halo orbits of the Hill problem seem not to be amenable to be stabilized by this mechanism. By increasing the characteristic length one never finds a reflection, and at certain value of ℓ it occurs the termination of the family onto an orbit of the family of eight-shaped orbits (see [5] for further details).

5 Conclusions

The attitude-orbit coupling that occurs in the case of satellites of non-negligible length may result in orbit stabilization in the unstable neighborhood of the L_2 collinear point. Specifically, our work establishes the existence and stability of periodic orbits associated with fast rotating elongated space structures. From a qualitative point of view, these orbits are the natural continuation of periodic motions typical of the Circular Restricted Three-Body Problem (Lyapunov, eight-shaped, and Halo orbits) whose dynamical characteristics are modified by the influence of the satellite's elongation. This fact suggests the use of space tethers as a purely dynamical stabilization mechanism.

Focusing on Halo orbits, the most promising regions to investigate are close to the stability region of the Hill problem. Notwithstanding, for real applications one needs also to check that the satellite's elongation required for stabilization is feasible with the actual technology.

Acknowledgements

Part of this research has been supported by Project AYA 2010-18796 of the Government of Spain.

References

1. Farquhar, R.W., Dunham, D.W., Guo, Y.P., McAdams, J. V., "Utilization of Libration Points for Human Exploration in the Sun-Earth-Moon System and Beyond," *Acta Astronautica*, Vol. 55, Nos. 3–9, 2004, pp. 687–700.
2. Simó, C., Gómez, G., Llibre, J., Martínez, R., "Station Keeping of a Quasiperiodic Halo Orbit Using Invariant Manifolds," in *Second International Symposium on Spacecraft Flight Dynamics*, pages 65–70. European Space Agency, Darmstadt, Germany, October 1986
3. Howell, K.C., Gordon, S.C., "Orbit Determination Error Analysis and a Station-Keeping Strategy for Sun-Earth L_1 Libration Point Orbits," *J. Astronautical Sciences*, Vol. 42, No. 2, 1994, pp. 207–228.
4. Gómez, G., Lo, M., Masdemont, J., Museth, K., "Simulation of Formation Flight Near Lagrange Points for the TPF Mission," *Advances in the Astronautical Sciences*, Vol. 109, No. 1, 2002, pp. 61–75.
5. Peláez, J., et al., *Dynamics and Stability of Tethered Satellites at Lagrangian Points*, Tech. Rept. 07-4201, Advanced Concept Team ESA, Nov. 2008.
6. Hénon, M., "Numerical Exploration of the Restricted Problem. V. Hill's Case: Periodic Orbits and Their Stability," *Astronomy and Astrophysics*, Vol. 1, 1969, pp. 223–238.
7. Gómez, G., Marcote, M., Mondelo, J.M., "The invariant manifold structure of the spatial Hill's problem," *Dynamical Systems: An International Journal*, Vol. 20, No. 1, 2005, pp. 115–147.
8. Peláez, J., et al., "Periodic orbits of the Hill-tether satellite problem originated from the L_2 collinear point," *J. of Guidance, Control and Dynamics*, submitted, Nov. 2010.

ℓ^2	Period	ξ	η	ζ	Type	k_1	k_2
0.0000000	3.6239341	0.58418481227642	-0.31241520606960	1.53290134575395	R	0.83462661E+03	0.16444627E+01
0.10941433	3.1882118	0.51714167003457	-0.41891935001911	1.81255377699810	R	0.299966633E+01	0.21810134E+01
0.10941596	3.1882336	0.51654757078963	-0.41947761744247	1.81390009020445	R	0.29319362E+01	0.19999996E+01
0.10920277	3.1919355	0.50934373490025	-0.42608861537005	1.83024120067338	R	0.20000000E+01	0.28280644E+00
0.10627519	3.2573626	0.48251090089231	-0.44561279167320	1.89496855832954	C	-0.19695846E+01	0.33979876E-06
0.10199785	3.3785750	0.45149481651980	-0.44646032120061	1.98750666824668	C	-0.19434455E+01	0.55755040E-07
0.09935360	3.4257057	0.43378298552662	-0.43514200002628	-2.05011375180728	R	0.20000000E+01	-0.15995007E-01
0.09476331	3.4488334	0.40789787574475	-0.41014256558719	2.15184482396913	R	0.13487390E+02	0.97530385E+01

Table 1: Relevant orbits in Fig. 3. From top to bottom: Starting orbit (1; Hill's problem); Minimum relative period (reflection in period); Maximum tether's length (2; reflection in ℓ); Change to stability; Change to complex instability (3); Change to stability (4); Change to real instability (5); and Maximum relative period (reflection in T)

ℓ^2	Period	ξ	ζ	η	Type	k_1	k_2
0.0000000	2.6012605	0.06764777158172	0.28816403555480	2.34254045571917	R	0.19005245E+02	-0.18733446E+01
0.00509202	2.3738229	0.02655502705041	0.22802231420218	2.57630987062592	R	0.20000002E+01	-0.14551250E+01
0.00426461	2.2445703	0.46456155161426	-0.80189538839854	-0.97766741251991	R	-0.61624752E+00	-0.20000000E+01
0.0000000	1.9171375	-0.00637109550814	0.11336157303427	4.04995510050092	R	0.93485373E+00	-0.36293316E+01

Table 2: Relevant orbits in Fig. 4. From top to bottom: Starting orbit (1; Hill's problem); Maximum tether's length (2; reflection in ℓ); Change to instability (3); Termination orbit (4; Hill's problem)